



## Osseointegration mechanisms: a proteomic approach

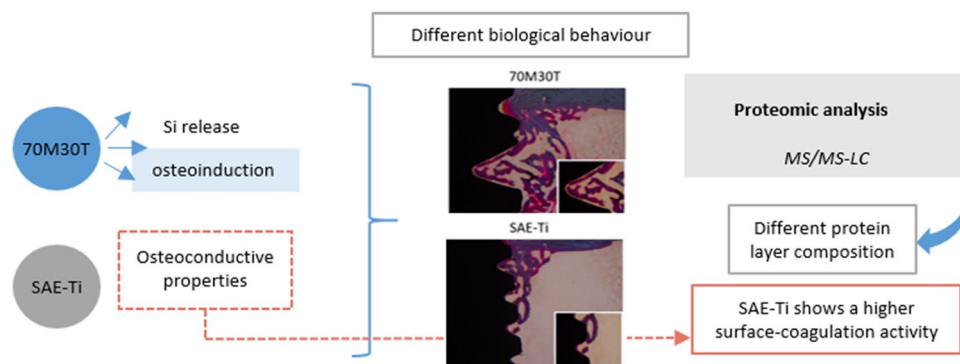
N. Araújo-Gomes<sup>1,2</sup> · F. Romero-Gavilán<sup>1</sup> · I. García-Arnáez<sup>3</sup> · C. Martínez-Ramos<sup>2</sup> · A. M. Sánchez-Pérez<sup>2</sup> · M. Azkargorta<sup>4</sup> · F. Elortza<sup>4</sup> · J. J. Martín de Llano<sup>5</sup> · M. Gurruchaga<sup>3</sup> · I. Goñi<sup>3</sup> · J. Suay<sup>1</sup>

Received: 18 January 2018 / Accepted: 19 March 2018 / Published online: 23 March 2018  
© SBIC 2018

### Abstract

The prime objectives in the development of biomaterials for dental applications are to improve the quality of osseointegration and to short the time needed to achieve it. Design of implants nowadays involves changes in the surface characteristics to obtain a good cellular response. Incorporating osteoinductive elements is one way to achieve the best regeneration possible post-implantation. This study examined the osteointegrative potential of two distinct biomaterials: sandblasted acid-etched titanium and a silica sol–gel hybrid coating, 70% MTMOS–30% TEOS. In vitro, in vivo, and proteomic characterisations of the two materials were conducted. Enhanced expression levels of ALP and IL-6 in the MC3T3-E1 cells cultured with coated discs, suggest that growing cells on such surfaces may increase mineralisation levels. 70M30T-coated implants showed improved bone growth in vivo compared to uncoated titanium. Complete osseointegration was achieved on both. However, coated implants displayed osteoinductive properties, while uncoated implants demonstrated osteoconductive characteristics. Coagulation-related proteins attached predominantly to SAE-Ti surface. Surface properties of the material might drive the regenerative process of the affected tissue. Analysis of the proteins on the coated dental implant showed that few proteins specifically attached to its surface, possibly indicating that its osteoinductive properties depend on the silicon delivery from the implant.

### Graphical abstract



**Keywords** Osteogenesis · Bone regeneration · Coagulation · Osteoinduction · Biointerfaces

### Introduction

Bone tissue undergoes continuous remodelling, which depends on the balance between the activities of highly specialised cells, the osteoblasts, and osteoclasts. This balance is adaptive; the system responds to mechanical stresses and

N. Araújo-Gomes and F. Romero-Gavilán were co-authorship.

✉ F. Romero-Gavilán  
gavilan@uji.es

Extended author information available on the last page of the article

is affected by the processes involved in the maintenance of bone health and bone regeneration [1].

The terms osteoinduction and osteoconduction are often used in the orthopedic field. They are commonly discussed in dental implantology practice, where various implants have been employed with long-term success rates of around 95% [2]. As the demand for this type of treatment is growing and the number of such surgeries is increasing, even these high rates seem to be insufficient. New surface types specifically designed for dental implants could improve the success ratios. They should also achieve better and faster osseointegration than the traditional materials [3]. This is especially important in cases with compromised bone regeneration capability (e.g., smokers, osteoporotic, and diabetic patients).

Osteoinduction (the process by which osteogenesis is induced) involves stimulation of undifferentiated cells, resulting in the development of bone-forming cell lineage [4]. Osteoconduction is the property of a material serving as a scaffold for the growth of bone tissue. The osteoconductive potential of a surface is affected by its roughness, microtopography, nanotopography, and porosity [5]. These two processes (osteoinduction and osteoconduction) are important for osseointegration, i.e., a direct structural and functional connection between the newly formed bone and the biomaterial [6].

The clinical success of a dental implant strongly depends on a short-term osseointegration. Good osseointegration rate of the titanium dental implants is necessary for a successful early clinical outcome [7]. Such implants, apart from supporting the correct healthy bone integration, should promote the activation of osteoblasts in the impaired tissue, stimulating the osteogenesis. This should facilitate surgical implantations in patients with regenerative limitations.

Thus, the design of new dental implants should consider both chemical and physical surface modifications. Such modifications affect surface implant topography, hydrophobicity and the chemical properties of the implant material (and especially, of its surface). The purpose is to enhance the biological interaction of the living tissue with the material [8].

The sol–gel hybrid materials synthesised using alkoxy-silanes are being increasingly used as coatings for biomedical applications. They are being developed as coatings for titanium dental implants [9, 10]. These biomaterials release silicic acid compounds ( $\text{Si}(\text{OH})_4$ ), which impart osteoinductive properties to the implant [11, 12].

The application of these coatings onto an implant surface affects its physical and chemical attributes, and, consequently, alters the conformation, type and quantity of proteins adsorbed immediately after implantation [13]. These are the proteins that might determine the initiation and intensity of the immune and inflammatory response and

coagulation [14] and activate processes triggering osteogenesis, leading to effective osseointegration. Thus, the studies of the adsorbed proteins primary importance for the orthopedics and other associated medical fields. Such studies should contribute to new insights into the mechanisms governing the microenvironment of the protein–biomaterial surface interactions. In particular, the use of proteomics is gaining additional interest and regarded as a novel strategy to assess bone healing process post-implantation [15].

This article presents *in vitro*, *in vivo*, and proteomic characterisations of two different surface types (SAE-Ti, and sol–gel coating). The bone regeneration mechanism and potential of the two surfaces are studied and compared.

## Materials and methods

### Titanium discs

Ti discs (Ti) (12 mm in diameter, 1 mm thick) were made from a bar of commercially available, pure, grade-4 Ti (Ilerimplant S.L., Lleida, Spain). To obtain the sandblasted, acid-etched (SAE) Ti, the discs were abraded with 4  $\mu\text{m}$  aluminium oxide particles and acid-etched by submersion in sulfuric acid for 1 h, to simulate a moderately rough implant surface. The discs were then washed with acetone, ethanol and 18.2  $\Omega$  purified water (for 20 min in each liquid) in an ultrasonic bath and dried under vacuum. Finally, all Ti discs were sterilised using UV radiation.

### Sol–gel synthesis and sample preparation

The silica hybrid sol–gel material was synthesised from the alkoxy-silane precursors: methyltrimethoxysilane (MTMOS) and tetraethyl orthosilicate (TEOS) (Sigma-Aldrich, St. Louis, MO, USA) in molar percentages of 70 and 30%, respectively. This composition was adopted on the basis of the previous results [9].

2-Propanol (Sigma-Aldrich, St. Louis, MO, USA) was used as a solvent in the process at a volume ratio (alcohol:siloxane) of 1:1. Hydrolysis of alkoxy-silanes was carried out by adding (at a rate of 1 drop  $\text{s}^{-1}$ ) the corresponding stoichiometric amount of 0.1 M aqueous solution of  $\text{HNO}_3$  (Panreac, Barcelona, Spain). The mixture was kept for 1 h under stirring followed by 1 h at rest. Coated samples were prepared immediately afterwards with SAE-Ti as a substrate. The samples were coated employing a KSV DC dip coater (Biolin Scientific, Stockholm, Sweden). Discs and implants were immersed in the sol–gel solution at a speed of 60  $\text{cm min}^{-1}$ , left immersed for 1 min, and removed at a 100  $\text{cm min}^{-1}$ . Finally, the samples were cured for 2 h at 80 °C.

## Physico-chemical characterisation of coated titanium discs

The surface topography of samples was examined by scanning electron microscopy (SEM), employing the Leica–Zeiss LEO equipment under vacuum (Leica, Wetzlar, Germany). Platinum sputtering was applied to make the materials more conductive. A mechanical profilometer Dektack 6M (Veeco Instruments, Plainview, NY, USA) was used to assess the material roughness. Two coated discs of each composition were tested. Three measurements were performed for each disc to obtain the average values of the Ra parameter. The contact angle was measured using an automatic contact angle meter OCA 20 (DataPhysics Instruments, Filderstadt, Germany). Aliquots of 10  $\mu\text{L}$  of ultrapure water W04 were deposited on the disc surfaces at a dosing rate of 27.5  $\mu\text{L s}^{-1}$  at room temperature. Contact angles were determined using the SCA 20 software. Six discs of each material were studied, after depositing two drops on each disc.

## In vitro assays

### Cell culture

Mouse calvaria osteosarcoma cells (MC3T3-E1) were cultured on the sol–gel-coated titanium discs at a concentration of  $1 \times 10^4$  cells/well. The cells were grown in Dulbecco's modified Eagle's medium (DMEM) with phenol red (Gibco-Life Technologies, Grand Island, NY, USA), 1% penicillin/streptomycin solution 100 $\times$  (Biowest Inc., Riverside, KS, USA), and 10% fetal bovine serum (FBS) (Gibco-Life Technologies). After incubation for 24 h at 37  $^\circ\text{C}$  in a humidified (95%) atmosphere with 5%  $\text{CO}_2$ , the medium was replaced with an osteogenic medium composed of DMEM with phenol red 1 $\times$ , 1% penicillin/streptomycin, 10% FBS, 1% ascorbic acid (5 mg  $\text{mL}^{-1}$ ) (Sigma-Aldrich), and 0.21%  $\beta$ -glycerol phosphate (Sigma-Aldrich), and incubated again under the same conditions. The culture medium was changed every 48 h. In each plate, an empty well with cells at the same concentration ( $1 \times 10^4$  cells) was used as a control of culture conditions. For RNA isolation, the cells were allowed to differentiate for 7 and 14 before being harvested.

### Cytotoxicity

The biomaterial cytotoxicity was evaluated following the ISO 10993-5 norm; it was assessed using spectrophotometry, after incubation of the cells with the material extract, obtained after following the norm. The CellTiter 96 Proliferation Assay (Promega<sup>®</sup>, Madison, WI, USA) was employed to measure cell viability after 24 h incubation. We used a negative control (the empty cell well) and a positive control with latex, known to be toxic to the cells. Seventy-percent

cell viability was the limit below which a biomaterial was considered cytotoxic.

### Cell proliferation

For measuring cell proliferation, the commercial cell-viability assay alamarBlue<sup>®</sup> (Invitrogen-Thermo Fisher Scientific, Waltham, MA, USA) was used. The kit measures the cell viability on the basis of a redox reaction with resazurin. The cells were cultured in wells with the discs (three replicates per treatment) and examined following the manufacturer's protocol after 1, 3, 5, and 7 days of culture. The results (percentage of reduced resazurin) were used to evaluate cell proliferation.

### Alkaline phosphatase (ALP) activity

The conversion of *p*-nitrophenylphosphate (*p*-NPP) to *p*-nitrophenol was used to assess the activity. The culture medium was removed from the wells, which were then washed three times with 1 $\times$  DPBS (Dulbecco's phosphate-buffered saline-ThermoFisher Scientific), and 100  $\mu\text{L}$  of lysis buffer (0.2% Triton X-100, 10 mM Tris–HCl, pH 7.2) (Sigma-Aldrich) was added to each well. Sample aliquots of 0.1 mL were used to conduct the assay. One hundred  $\mu\text{L}$  of *p*-NPP (1 mg  $\text{mL}^{-1}$ ) in substrate buffer (50 mM glycine, 1 mM  $\text{MgCl}_2$ , pH 10.5) was added to 100  $\mu\text{L}$  of the supernatant obtained from the lysate. After 2 h of incubation in the dark (37  $^\circ\text{C}$ , 5%  $\text{CO}_2$ ), the absorbance was measured, using a microplate reader, at a wavelength of 405 nm. ALP activity was read from a standard curve obtained using different solutions of *p*-nitrophenol and 0.02 mM sodium hydroxide (Sigma-Aldrich). The results were presented as mmol of *p*-nitrophenol/hour (mmol PNP  $\text{h}^{-1}$ ). The data were expressed as ALP activity normalized to the total protein content ( $\mu\text{g } \mu\text{L}^{-1}$ ) obtained using Pierce BCA assay kit (Thermo Fisher Scientific, Waltham, MA, USA) after 7 and 14 days of culture.

### RNA isolation and cDNA synthesis

Total RNA was prepared from the cell lysates grown on the sol–gel-coated titanium discs, using Qiagen RNeasy Mini kit (Hilden, Germany), following digestion with DNase I (Qiagen), according to the manufacturer's instructions. The quantity, integrity, and quality of the resulting RNA were assessed using NanoVue<sup>®</sup> Plus Spectrophotometer (GE Healthcare Life Sciences, Little Chalfont, United Kingdom). For each sample, approximately 1  $\mu\text{g}$  of total RNA was converted to cDNA using PrimeScript RT Reagent Kit (Perfect Real Time) (TAKARA Bio Inc., Shiga, Japan). The resulting cDNA was diluted in DNase-free water to a concentration suitable for reliable RT-PCR analysis.

## Quantitative real-time PCR

Before the qRT-PCR reaction, primers for ALP, IL6, Col I, and OCN genes were designed from specific DNA sequences available from NCBI (<https://www.ncbi.nlm.nih.gov/nucleotide>), using PRIMER3plus software tool (<http://www.bioinformatics.nl/cgi-bin/primer3plus/primer3plus.cgi>). Expression levels were measured using primers purchased from Life Technologies S.A. (Gaithersburg, MD); GADPH sense, TGCCCCCATGTTTGTGATG; GADPH antisense, TGGTGGTGCAGGATGCATT; alkaline phosphatase sense, CCAGCAGGTTTCTCTCTTGG; alkaline phosphatase antisense, CTGGGAGTCTCATCCTGAGC; IL6 sense, AGTTGCCTTCTGGGACTGA; IL6 antisense, TCCACGATTTCCAGAGAAC; COLIA1 sense, CCTGGTAAA GATGGTGCC; COLI antisense, CACCAGGTTACCTTTCGCACC; OCN sense, GAACAGACTCCGGCGCTA and OCN antisense, AGGGAGGATCAAGTCCCG. All primers are listed from 5' to 3'. GADPH was used as a housekeeping gene to normalize the data obtained from the qRT-PCR and calculate the relative fold change between the conditions. qPCR reactions were carried out using SYBR Premix Ex Taq (Tli RNase H Plus) (TAKARA), in a StepOne Plus™ Real-Time PCR System (Applied Biosystems, Foster City, California, USA). The cycling parameters were as follows: an initial denaturation step at 95 °C for 30 s; followed by 95 °C for 5 s and 60 °C for 34 s for a total of 40 cycles. The final melt curve stage comprised a cycle of 95 °C for 15 s and 60 °C for 60 s.

## Statistical analysis

Data were submitted to one-way analysis of variance (ANOVA) and to a Newman–Keuls multiple comparison post-test, when appropriate. Differences with  $p \leq 0.05$  were considered statistically significant.

## In vivo experimentation

The in vivo procedures and histological evaluation of the two tested materials, SAE-Ti and 70M30T, were carried out using the previously described methods [9], with the tibia of New Zealand rabbits (*Oryctolagus cuniculus*) as the experimental model. All the experiments were conducted in accordance with the protocols of Ethical Committee of the Valencia Polytechnic University (Spain), the European guidelines and legal conditions in R. D. 223/1988 of March 14th, and the Order of October 13th, 1988 of the Spanish Government on the protection of animals used for experimentation and other scientific purposes. Briefly, the dental implants, supplied by Ilerimplant S.L. (Lleida, Spain), were the Frontier model (3.75 mm diameter and 8 mm length) with SAE surface treatment. Twenty implants were used, 10

uncoated (SAE-Ti) and 10, coated (70M30T). The implantation periods of the experimental model were 2 and 4 weeks. Five rabbits were used for each material; the implants were inserted into the tibiae of the animals. The samples for histological examination were embedded in methyl methacrylate using EXAKT technique (EXAKT Technologies, Inc., Oklahoma, USA). For optical microscopy examination, all the sections were stained using Gomori Trichrome solution.

## Adsorbed protein layer

Both 70M30T-coated and uncoated SAE titanium discs were incubated in a 24-well plate for 180 min in a humidified atmosphere (37 °C, 5% CO<sub>2</sub>), after the addition of 1 mL of human blood serum from male AB plasma (Sigma-Aldrich, St. Louis, MO, USA).

The serum was removed, and, to eliminate the non-adsorbed proteins, the discs were rinsed five times with ddH<sub>2</sub>O and once with 100 mM NaCl, 50 mM Tris–HCl, pH 7.0. The adsorbed protein layer was collected by washing the discs in 0.5 M triethylammonium bicarbonate buffer (TEAB) with 4% of sodium dodecyl sulphate and 100 mM dithiothreitol (Sigma-Aldrich). Four independent experiments were carried out for each coating ( $n = 4$ ); in each experiment, each elution was obtained from the incubation of serum of four discs, for each formulation. The protein content was quantified (Pierce BCA assay kit; Thermo Fisher Scientific), obtaining a value of 51 mg mL<sup>-1</sup>.

## Proteomic analysis

Proteomic analysis was performed as described by Romero-Gavilán et al. [16], with minor variations. Briefly, the eluted protein was resolved in polyacrylamide gels; then, the bands were cut out. Each of the slices was digested with trypsin and loaded onto a nanoACQUITY UPLC system connected online to an SYNAPT G2-Si MS System (Waters, Milford, MA, USA). Each material was analysed in quadruplicate. Differential protein analysis was carried out using Progenesis software (Nonlinear Dynamics, Newcastle, UK) as described before [16]. The functional annotation of the identified differential proteins was performed using PANTHER (<http://www.pantherdb.org>) and DAVID Go annotation programmes (<https://david.ncifcrf.gov/>).

## Results

### Synthesis and physico-chemical characterisation

Scanning electron microscopy micrographs (Fig. 1) demonstrated that the sol–gel preparation was carried out correctly and a homogenous coating was obtained. Some

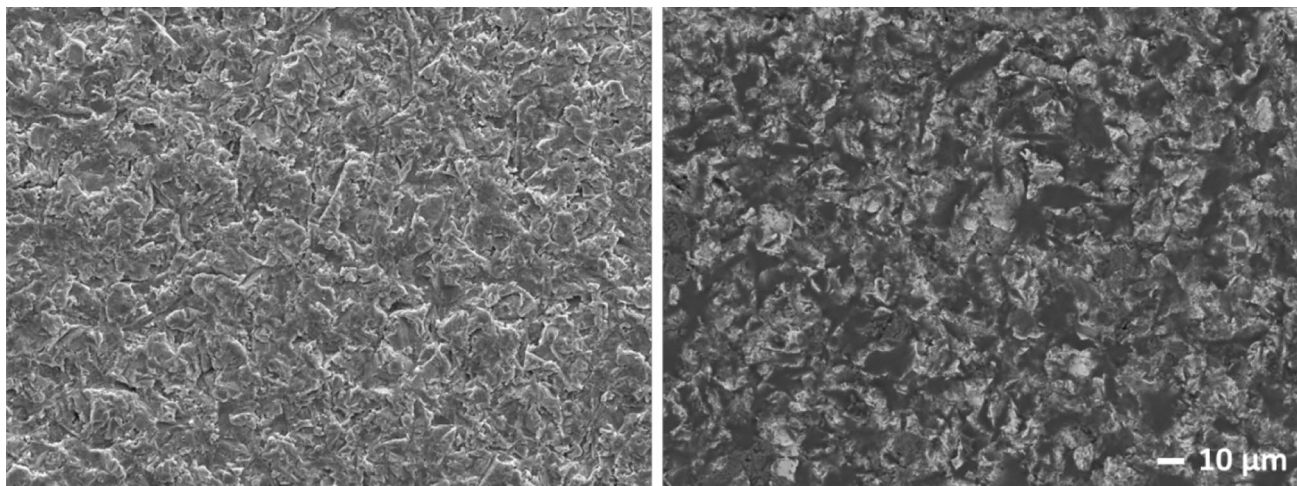


**Fig. 1** SEM micrographs of SAE-Ti surfaces and 70M30T sol-gel coating. Calibration bar 10  $\mu\text{m}$

morphological differences between the SAE-Ti surfaces and 70M30T coatings were observed; the initial SAE-Ti roughness was diminished after coating. The Ra, measured using a mechanical profilometer, was lower for the coated samples. The Ra for SAE-Ti was  $0.98 \pm 0.09 \mu\text{m}$  and for 70M30T sol-gel coating,  $0.87 \pm 0.13 \mu\text{m}$ . The sol-gel treatment also caused a decrease in the contact angle. The angle was  $79.55^\circ \pm 7.51^\circ$  for SAE-Ti and  $50.78^\circ \pm 1.82^\circ$  for 70M30T, showing a significant increase in hydrophilicity after coating.

## In vitro assays

### Cytotoxicity, proliferation, and ALP activity

Neither of the tested materials was cytotoxic (data not shown). Cell proliferation results did not show significant differences between the tested materials (Fig. 2a). There were no differences between ALP activities for the two materials after 7 and 14 days of incubation (Fig. 2b).

### mRNA expression levels

The mRNA expression levels for ALP and IL-6 genes show a distinctive and significant response of the osteoblasts to the coating. After 14 days of culture, the expression of these genes was substantially higher for the cells grown on the

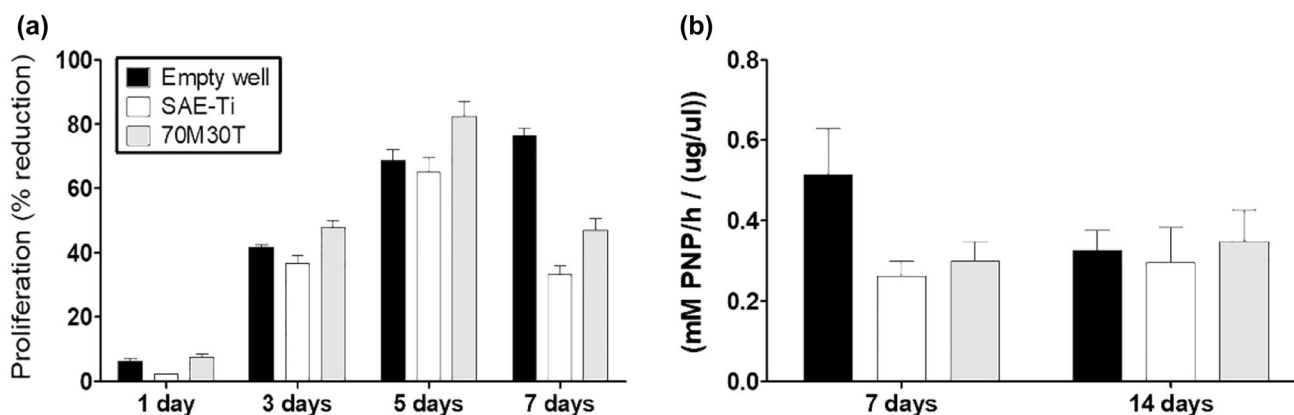


**Fig. 2** MC3T3-E1 in vitro assays: **a** MC3T3-E1 cell proliferation after 1, 3, 5, and 7 days of incubation with SAE-Ti (white bar) and 70M30T (grey bar) materials. **b** ALP activity ( $\text{mM PNP/h} / (\mu\text{g} \mu\text{L}^{-1})$ ) normalized to the amount of total protein ( $\mu\text{g} \mu\text{L}^{-1}$ ) levels in the MC3T3-E1

cells cultivated on SAE-Ti (white bar) and 70M30T formulation (grey bar). Cells incubated without discs were used as a positive control (black bar)



coated surfaces than on the non-coated titanium (Fig. 3a, b). These results suggest an enhanced cell mineralisation when cultured on the coated implants [17, 18].

COL I expression was similar for the two materials throughout the experiment. After 7 days of culture, the OCN expression levels were significantly higher for the non-coated titanium than for the coated surfaces (Fig. 3c, d). OCN is a pre-osteoblastic marker; its diminished expression levels on the 70M30T surfaces support the hypothesis that the sol–gel material accelerates the osteogenesis processes [19].

### In vivo experimentation

The results of in vivo experiments showed similar regeneration behaviours for the two implants tested. SAE-Ti implants displayed, as expected, good osteointegration after 2 and 4 weeks (Fig. 4). In some of the roots of the threads of the 70M30T-coated implants, an unstained material corresponding to the remaining sol–gel coating was observed. The 70M30T implants also showed good osteointegrative properties, and qualitatively, the osteogenic activity seemed higher than on the SAE-Ti surfaces. As shown in Fig. 5,

70M30T-coated surface induced the growth of new bone tissue spicules from the cortical region into the medullary cavity.

### Proteomic analysis

The LC–MS/MS analysis identified 113 proteins. The statistical comparison of the results obtained for SAE-Ti and 70M30T materials was carried out using the Progenesis QI software. The DAVID and PANTHER programmes were employed to classify the detected proteins according to their function.

The comparison between the proteins identified on the two tested materials revealed that only 1 protein preferentially adsorbed onto the 70M30T surface (CLUS, classified as a glycoprotein by DAVID). However, 31 proteins favoured the SAE-Ti (Table 1). Within this group, a large number of lipoproteins were found, such as apolipoproteins APOA2, APOA5, APOC1, APOC3, APOC4, APOE, APOL1, and the SAA4, a high-density lipoprotein particle. Several proteins associated with blood coagulation functions were also identified. The coagulation factors FA5, FA10 and FA11, THR3, ANT3, PLMN, PROC and PROS belong to this set

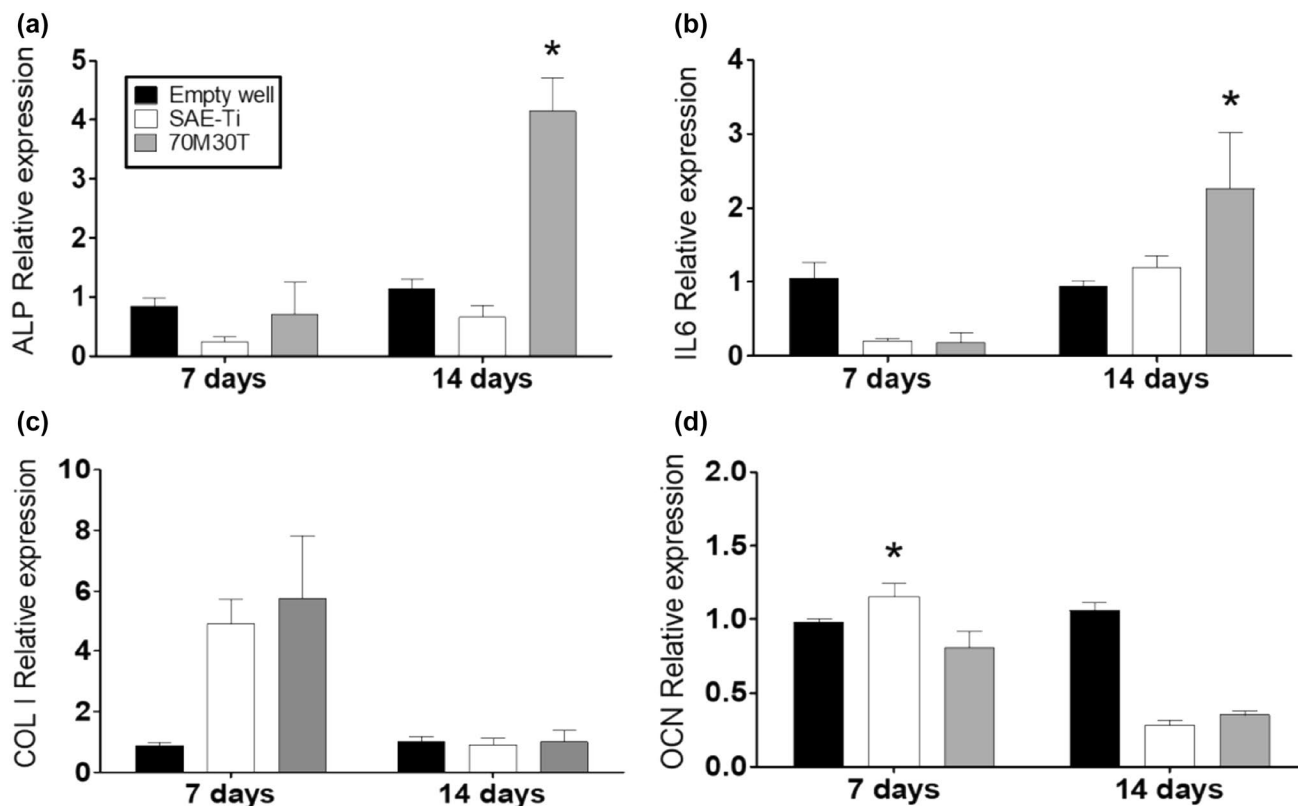


**Fig. 3** Gene expression of osteogenic markers **a** ALP, **b** IL6, **c** COL I, and **d** OCN in MC3T3-E1 osteoblastic cells cultured on SAE-Ti (white bar) and 70M30T (grey bar). The relative mRNA expression

was determined by RT-PCR after 7 and 14 days of culture. Statistical analysis was performed using one-way ANOVA with a Kruskal–Wallis post-test ( $*p \leq 0.05$ )

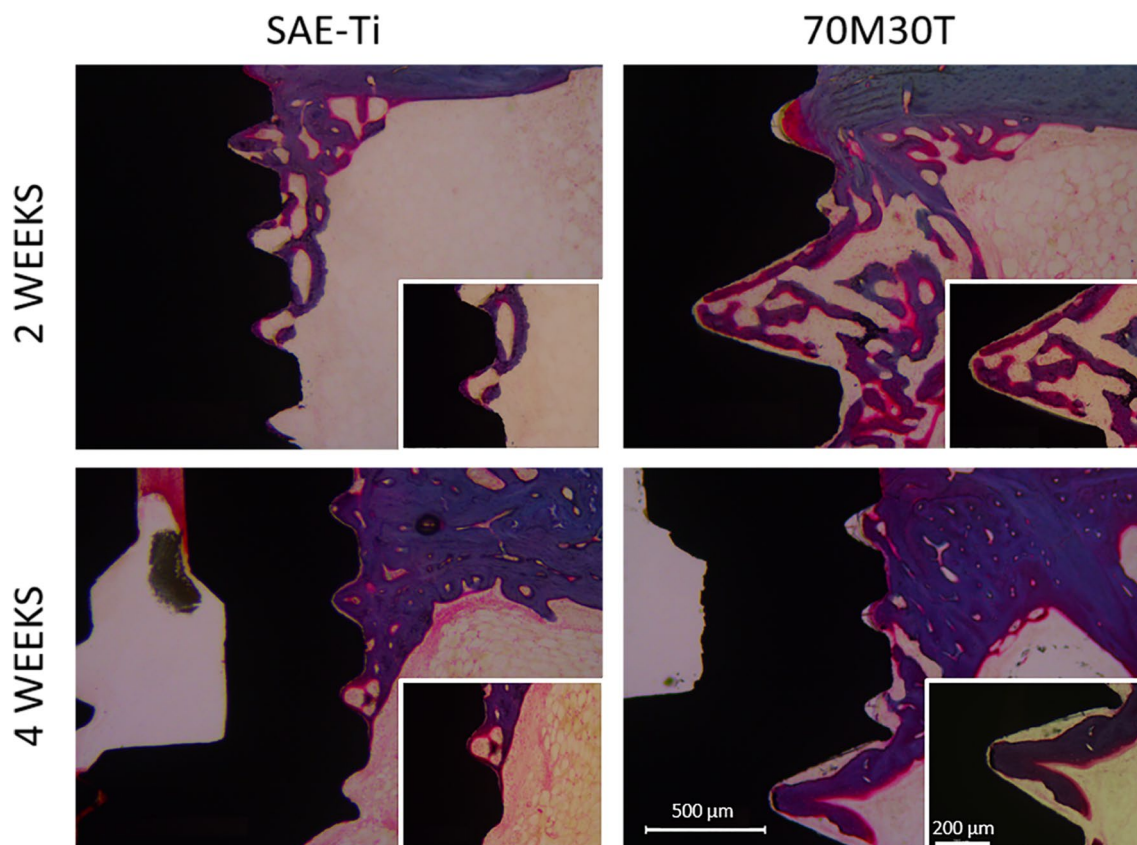


**Fig. 4** Microphotographs of samples of SAE-Ti and 70M30T implants. The main panels show  $\times 4$  magnification images of regions close to the cortical bone (up) and the bone marrow cavity (down). The lower right insets represent regions of interest

of proteins. Moreover, DAVID listed HRG, PLMN, PROS, THRB, and KLKB1 as proteins involved in fibrinolysis process. TETN, SEPP1, PF4 V, and VTNC were classified as glycoproteins. Intracellular proteins such as keratins K2C3, K22O, K2C1B, and K2C4 were also found.

The PANTHER pie chart in Fig. 6 shows the functional classification of the proteins adhering more to the SAE-Ti than to 70M30T surface. The most common biological functions were related to cellular processes (19%), biological regulation (14%) and response to stimulus (14%). Notably, a proportion of associated functions were represented by the immune system processes (3%). Among the proteins linked to various pathway processes, 84% were associated with blood coagulation. Two small groups of proteins (8%) were linked to the plasminogen activating cascade and inflammation.

## Discussion

In the recent years, improving the bioactivity of materials has become an utmost standard field of study for biomaterial studies, in particular in the field of dental science.

The successful incorporation of an implant into a living organism involves a series of unknown biological mechanisms, including processes like coagulation and immune response, leading to a desired correct bone regeneration [20]. These processes are triggered by the first layer of proteins adsorbed on the biomaterial surfaces, conditioning and determining cell behaviour during the post-implantation recovery [14]. After a surgical procedure, there are some immediate interactions between those proteins and the biomaterial. The extent and type of these interactions largely depend, apart from the biochemistry of the organism, on the physical and chemical surface characteristics of the implant. These characteristics often determine a specific type, quantity and conformation of the proteins attaching to the implant surface via competitive displacement, known as the Vroman effect [21]. Hence, this experimental work focused on the interactions between the implant surface and serum proteins.

The intrinsic physico-chemical characteristics of the tested surfaces can condition the cellular behaviour and, consequently, modulate the adaptation to the implanted foreign body. The analysis of the materials examined here showed clear differences between their chemical composition and

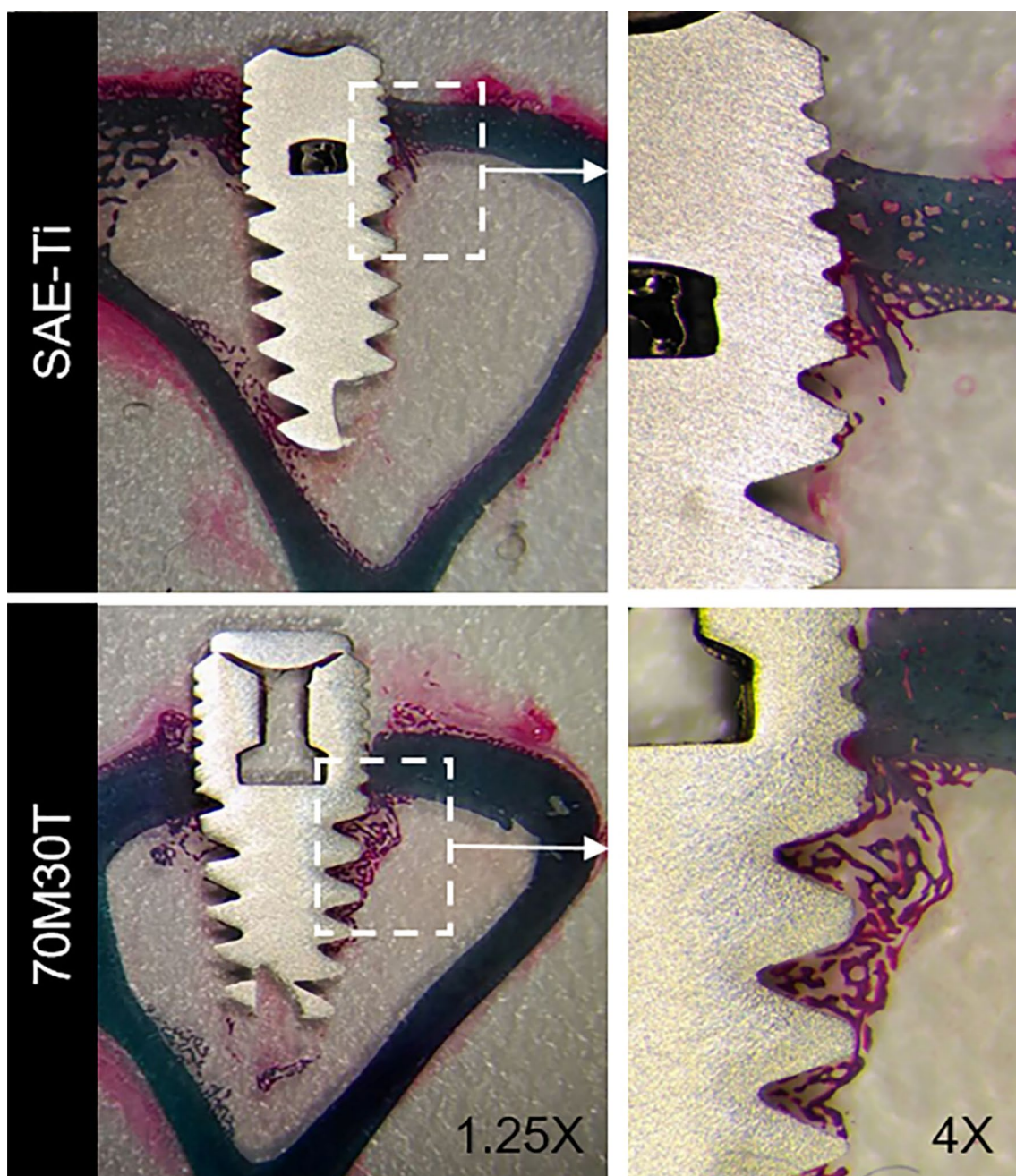


**Fig. 5** Bone tissue growth 4 weeks after implantation. Panoramic (left) and detailed (right) microphotographs of SAE-Ti and 70M30T implants show the bone tissue generated around the implant surface

physico-chemical properties (hydrophilicity, topography and contact angle).

These differences were not unexpected given the characteristic, distinct cell behaviour in response to each surface type. The 70M30T coating triggered stronger cell responses, particularly noticeable on the mRNA expression levels. The expression of ALP and IL-6, the major biomarkers of osteogenic differentiation [17, 18], was enhanced in the cells exposed to the coated surface in

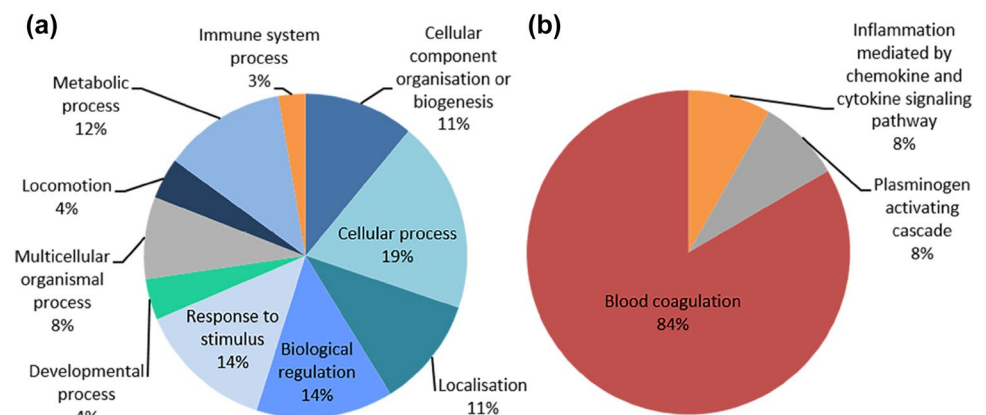
comparison with the uncoated SAE-Ti surfaces. The difference was sufficiently significant to infer that this coating affected the cell behaviour.

However, in the *in vivo* experiments, these differences were not so clear-cut (Fig. 4). These results suggest that the processes underlying the osseointegration for these two surface types are distinct or regulated by different mechanisms (Fig. 5).



**Table 1** Proteins differentially attached to 70M30T and Ti (progenesis analysis)

Description	Accession	Confidence score	Anova ( <i>p</i> )	Normalized abundance		
				Average 70M30T	Average Ti	Ratio Ti/70M30T
Clusterin	CLUS_HUMAN	596.70	3.95E-03	7.50E+05	4.89E+05	0.65
Keratin, type II cytoskeletal 3	K2C3_HUMAN	263.73	4.64E-02	2.60E+05	3.09E+05	1.19
Keratin, type II cytoskeletal 2 oral	K22O_HUMAN	223.71	4.37E-02	3.54E+05	4.22E+05	1.19
Keratin, type II cytoskeletal 1b	K2C1B_HUMAN	292.46	7.61E-03	4.81E+03	6.41E+03	1.33
Apolipoprotein C-III	APOC3_HUMAN	212.82	4.42E-02	4.51E+05	7.69E+05	1.71
Apolipoprotein L1	APOL1_HUMAN	235.45	8.28E-04	9.45E+04	1.64E+05	1.73
Plasminogen	PLMN_HUMAN	781.12	1.62E-02	2.36E+05	4.32E+05	1.83
Ig lambda chain V-III region SH	LV301_HUMAN	120.13	1.25E-02	3.67E+04	7.51E+04	2.05
Coagulation factor V	FA5_HUMAN	192.62	2.04E-05	9.83E+03	2.04E+04	2.08
Apolipoprotein A-V	APOA5_HUMAN	194.49	1.14E-03	8.91E+03	2.41E+04	2.70
Vitamin K-dependent protein S	PROS_HUMAN	78.23	9.83E-03	4.21E+03	1.20E+04	2.85
Ig kappa chain V-III region SIE	KV302_HUMAN	153.44	5.26E-03	8.45E+04	2.56E+05	3.03
Plasma kallikrein	KLKB1_HUMAN	86.19	1.60E-04	2.91E+03	9.45E+03	3.24
Tetranectin	TETN_HUMAN	206.13	3.01E-03	8.11E+03	2.72E+04	3.35
Selenoprotein P	SEPP1_HUMAN	208.07	2.92E-05	1.94E+04	6.99E+04	3.60
Apolipoprotein A-II	APOA2_HUMAN	144.49	1.00E-03	6.31E+04	2.77E+05	4.39
Antithrombin-III	ANT3_HUMAN	488.69	3.49E-04	6.55E+04	3.14E+05	4.80
Apolipoprotein E	APOE_HUMAN	1831.27	5.56E-07	1.82E+06	9.32E+06	5.11
Prothrombin	THRB_HUMAN	369.68	9.15E-04	4.62E+04	2.77E+05	5.99
Keratin, type II cytoskeletal 4	K2C4_HUMAN	155.48	1.60E-02	8.74E+02	5.76E+03	6.59
Serum amyloid A-4 protein	SAA4_HUMAN	135.14	7.04E-04	4.94E+04	3.45E+05	6.98
Kininogen-1	KNG1_HUMAN	350.85	6.48E-06	5.49E+04	4.16E+05	7.59
Coagulation factor XI	FA11_HUMAN	296.94	1.56E-05	1.78E+04	1.96E+05	11.00
Platelet basic protein	CXCL7_HUMAN	82.00	1.28E-06	2.48E+03	2.90E+04	11.70
Apolipoprotein C-I	APOC1_HUMAN	185.56	9.22E-08	2.51E+05	2.97E+06	11.81
Apolipoprotein C-IV	APOC4_HUMAN	96.41	3.11E-06	6.24E+03	7.86E+04	12.60
Creatine kinase M-type	KCRM_HUMAN	146.67	2.33E-05	9.78E+02	2.26E+04	23.08
Histidine-rich glycoprotein	HRG_HUMAN	527.94	4.86E-07	3.90E+04	9.09E+05	23.33
Coagulation factor X	FA10_HUMAN	81.54	5.51E-06	8.72E+02	2.31E+04	26.53
Vitamin K-dependent protein C	PROC_HUMAN	70.62	1.74E-03	1.90E+02	5.96E+03	31.28
Vitronectin	VTNC_HUMAN	307.15	3.10E-03	7.52E+04	2.99E+06	39.76
Platelet factor 4 variant	PF4V_HUMAN	117.94	2.64E-05	3.19E+02	2.68E+05	840.27

ANOVA (*p* value < 0.05)**Fig. 6** PANTHER pie charts with the biological process (a) and pathway (b) functions for the proteins adhering predominantly to SAE-Ti in comparison with 70M30T surfaces. These percentages are in regard of the specific function frequencies in the differential proteins

In the case of SAE-Ti, the regeneration process might be based on osteoconduction, while the bone repair achieved using the 70M30T implants might be primarily based on osteoinduction. The differences between the compositions of the respective protein layers suggest a correlation between the attached proteins and the particular mechanism of bone regeneration. The examination of the proteins adsorbed onto different surfaces might help to find this correlation.

Only one protein, CLUS, was adsorbed preferentially to the 70M30T-coated surface. This protein has been associated with several functions. Among those, there are some processes with a role in inflammation and immunity, such as the regulatory activity of complements [22]. In contrast, 31 proteins were significantly and predominantly attached to the SAE-Ti surface. A substantial number of apolipoproteins were part of this group. Apolipoproteins, besides their function in lipid metabolism, might prevent the initiation of innate immunity [23]. Immunoglobulins LV301 and KV302 were two of the characteristic proteins attached to the titanium surface; this could be related to the immune system process functions (3%) shown in Fig. 6. Although the proteomic study was carried out using human serum, some intracellular proteins such as keratins were obtained during the elution. The presence of these molecules could be an artefact of the industrial process used to purify the serum. According to DAVID classification, some of the proteins with more affinity to SAE-Ti than to 70M30T (HRG, PLMN, PROS, THRB and KLKB1) are involved in the fibrinolysis process. These proteins, as well as FA5, FA10, FA11, PROC, ANT3 and KNG1, are also related to the coagulation system. The PANTHER classification (pathway functions) indicates that 84% of the proteins preferentially adhering to SAE-Ti are associated with the blood coagulation (Fig. 6). Both fibrinolysis and coagulation are the processes necessary to achieve a correct bone tissue repair [24]. Among the SAE-Ti-associated proteins, FA5, FA10, FA11 and THBR might play a role in blood coagulation pathway, promoting blood clotting. ANT III, PROC and PROS are involved in the regulation of this pathway [25]. PLMN has an important role in the plasminogen system activation, the key step in the fibrinolysis process. After trauma, the coagulation system is one of the main initiators of the development of blood clots. Following this event, the plasminogen system acts during the extracellular matrix degradation and the consequent tissue remodelling and angiogenesis, leading to correct tissue healing [26]. The HRG protein is associated with blood coagulation, fibrinolysis and innate immune systems. It could function as both anticoagulant and antifibrinolytic modulator and might regulate platelet function *in vivo* [27]. KLKB1 is involved in the regulation of multiple proteolytic cascades, such as the intrinsic pathway of coagulation, as well as the fibrinolytic system and the complement pathways [28]. In addition, KLKB1, in association with FA12 and

high-molecular-weight KNG1, forms the kinin–kallikrein surface-activated coagulation system [29].

Some of the SAE-Ti-attached proteins, such as VTNC, TETN and APOE, might have osteogenic activity. APOE has a role in the vitamin K uptake into osteoblasts [30]. VTNC could promote the human osteoblast attachment and proliferation on the Ti implants, accelerating the osseointegration process [31]. The TETN protein has been linked to correct bone tissue development; TETN-knock-out mice have kyphosis and show the symptoms of osteoporosis [32].

On the basis of the available data and the *in vitro* and *in vivo* results obtained here, it is tempting to suggest a relationship between the type and function of these proteins and different mechanisms of osseointegration *in vivo*. The 70M30T material, releasing Si compounds into the implant surroundings might stimulate the undifferentiated osteoblasts, leading to the formation of bone tissue [33, 34]. This would represent a case of osteoinduction in the tissue surrounding the implant; such assumption is supported by the overexpression of osteogenesis-related genes, ALP and IL-6, demonstrated here. This mechanism could not be proven by the proteomic analysis of the eluate from the implant surface.

However, the predominance of coagulation- and fibrinolysis-related proteins adsorbed onto the SAE-Ti surface could indicate an ongoing osteoconduction process with the participation of key proteins such as PLMN and VTNC. This result illustrates the validity of the proteomic analysis, reflecting the *in vivo* outcome. Moreover, the coagulation might be the result of the kallikrein–kinin system activation. This is consistent with the hypothesis that the coagulation and, consequently, the regeneration, spreading from the titanium surface to the medullar area of the implanted bone, are based on an osteoconductive process.

## Conclusions

Two different dental implants, sandblasted acid-etched titanium (SAE-Ti) and a silica sol–gel hybrid coating (70M30T), were characterised. The results suggest two different mechanisms of bone regeneration. The SAE-Ti surfaces display osteoconductive properties. However, the *in vivo* results for silica sol–gel implants suggest osteoconductive behaviour. These results were confirmed by *in vitro* testing. The 70M30T coating displayed strong cell activation properties. The mRNA expression levels for ALP and IL-6, important biomarkers of osteogenic differentiation, were higher for 70M30T than for SAE-Ti surfaces. The results of proteomic analysis could explain some differences observed in bone healing. In particular, the effect of surface properties on cell behaviour could shed some light on the osteoconduction phenomenon. It is tempting to infer that certain proteins

related to coagulation processes take part in the initial regenerative events on the biomaterial surface.


**Acknowledgements** This work was supported by MAT2017-86043-R (MINECO); Universidad Jaume I under UJI-B2017-37 and Grant Predoc/2014/25; University of the Basque Country (UPV/EHU) through UFI11/56; Basque Government through IT611-13 and Grant Predoc/2016/1/0141, and Generalitat Valenciana under Grant Grisolia/2014/016. Authors would like to thank Antonio Coso and Jaime Franco (GMI-Ilerimplant) for their inestimable contribution to this study, and Raquel Oliver, José Ortega (UJI) and Iraide Escobes (CIC bioGUNE) for their valuable technical assistance.

## References

- Khan WS, Rayan F, Dhinsa BS, Marsh D (2012) An osteoconductive, osteoinductive, and osteogenic tissue-engineered product for trauma and orthopaedic surgery: how far are we? *Stem Cells Int*. Article ID 236231, 7. <https://doi.org/10.1155/2012/236231>
- Charyeva O, Altynbekov K, Zhartybaev R, Sabdanaliev A (2012) Long-term dental implant success and survival—a clinical study after an observation period up to 6 years. *Swed Dent J* 36:1–6
- Le Guéhennec L, Soueidan A, Layrolle P, Amouriq Y (2007) Surface treatments of titanium dental implants for rapid osseointegration. *Dent Mater* 23:844–854. <https://doi.org/10.1016/j.denta.1.2006.06.025>
- Solheim E (1998) Osteoinduction by demineralised bone. *Int Orthop* 22:335–342. <https://doi.org/10.1007/s002640050273>
- Wilson-Hench J (1987) Osteoinduction. In: Williams DF (ed) *Progress in biomedical engineering, Defin Biomater*, vol 4. Elsevier, p 29
- Carlsson L, Röstlund T, Albrektsson B et al (1986) Osseointegration of titanium implants. *Acta Orthop Scand* 57:285–289. <https://doi.org/10.3109/17453678608994393>
- Eckert SE, Koka S (2006) Osseointegrated dental implants. In: Johnson FE, Virgo KS, Lairmore TC, Audisio RA (eds) *The bionic human*, Humana Press. [https://doi.org/10.1007/978-1-59259-975-2\\_45](https://doi.org/10.1007/978-1-59259-975-2_45)
- Buser D, Brogini N, Wieland M et al (2004) Enhanced bone apposition to a chemically modified SLA titanium surface. *J Dent Res* 83:529–533. <https://doi.org/10.1177/154405910408300704>
- Martinez-Ibañez M, Juan-Díaz MJ, Lara-Saez I et al (2016) Biological characterization of a new silicon based coating developed for dental implants. *J Mater Sci Mater Med* 27:80. <https://doi.org/10.1007/s10856-016-5690-9>
- Romero-Gavilán F, Barros-Silva S, García-Cañadas J et al (2016) Control of the degradation of silica sol-gel hybrid coatings for metal implants prepared by the triple combination of alkoxysilanes. *J Non Cryst Solids* 453:66–73. <https://doi.org/10.1016/j.jnoncrysol.2016.09.026>
- Reffitt DM, Ogston N, Jugdaohsingh R et al (2003) Orthosilicic acid stimulates collagen type 1 synthesis and osteoblastic differentiation in human osteoblast-like cells in vitro. *Bone* 32:127–135. [https://doi.org/10.1016/S8756-3282\(02\)00950-X](https://doi.org/10.1016/S8756-3282(02)00950-X)
- Ha SW, Neale Weitzmann M, Beck GR (2014) Bioactive silica nanoparticles promote osteoblast differentiation through stimulation of autophagy and direct association with LC3 and p62. *ACS Nano* 8:5898–5910. <https://doi.org/10.1021/nn5009879>
- Schmidt DR, Waldeck H, Kao WJ (2009) Protein adsorption to biomaterials. In: Puleo DA, Bizios R (eds) *Biological interactions on materials surfaces: understanding and controlling protein, cell, and tissue*, Springer. <https://doi.org/10.1007/978-0-387-98161-1>
- Chen Z, Klein T, Murray RZ et al (2015) Osteoimmunomodulation for the development of advanced bone biomaterials. *Mater Today* 19:304–321. <https://doi.org/10.1016/j.matod.2015.11.004>
- Calciolari E, Donos N (2018) The use of omics profiling to improve outcomes of bone regeneration and osseointegration. How far are we from personalized medicine in dentistry? *J Proteomics*. <https://doi.org/10.1016/j.jprot.2018.01.017>
- Romero-Gavilán F, Gomes NC, Ródenas J et al (2017) Proteome analysis of human serum proteins adsorbed onto different titanium surfaces used in dental implants. *Biofouling* 33:98–111. <https://doi.org/10.1080/08927014.2016.1259414>
- Ajai S, Sabir A (2013) Evaluation of serum alkaline phosphatase as a biomarker of healing process progression of simple diaphyseal fractures in adult patients. *Int Res J Biol Sci Int Res J Biol Sci* 2:2278–3202
- Li Y, Bäckesjö C-M, Haldosén L-A, Lindgren U (2008) IL-6 receptor expression and IL-6 effects change during osteoblast differentiation. *Cytokine* 43:165–173. <https://doi.org/10.1016/j.cyto.2008.05.007>
- Huang W, Yang S, Shao J, Li Y-P (2007) Signaling and transcriptional regulation in osteoblast commitment and differentiation. *Front Biosci* 12:3068–3092. <https://doi.org/10.2741/2296>
- Al-maawi S, Orłowska A, Sader R et al (2017) In vivo cellular reactions to different biomaterials—physiological and pathological aspects and their consequences. *Semin Immunol* 29:49–61. <https://doi.org/10.1016/j.smim.2017.06.001>
- Hirsh SL, McKenzie DR, Nosworthy NJ et al (2013) The Vroman effect: competitive protein exchange with dynamic multilayer protein aggregates. *Colloids Surf B Biointerfaces* 103:395–404. <https://doi.org/10.1016/j.colsurfb.2012.10.039>
- Falgarone G, Chiochia G (2009) Clusterin: a multifacet protein at the crossroad of inflammation and autoimmunity. *Adv Cancer Res* 104:139–170. [https://doi.org/10.1016/S0065-230X\(09\)04008-1](https://doi.org/10.1016/S0065-230X(09)04008-1)
- Cho NH, Seong SY (2009) Apolipoproteins inhibit the innate immunity activated by necrotic cells or bacterial endotoxin. *Immunology* 128:479–486. <https://doi.org/10.1111/j.1365-2567.2008.03002.x>
- Loi F, Córdova LA, Pajarinen J et al (2016) Inflammation, fracture and bone repair. *Bone* 86:119–130. <https://doi.org/10.1016/j.bone.2016.02.020>
- Chu AJ (2010) Blood coagulation as an intrinsic pathway for proinflammation: a mini review. *Inflamm Allergy Drug Targets* 9:32–44. <https://doi.org/10.2174/187152810791292890>
- Wehner C, Janjić K, Agis H (2017) Relevance of the plasminogen system in physiology, pathology, and regeneration of oral tissues—from the perspective of dental specialties. *Arch Oral Biol* 74:136–145. <https://doi.org/10.1016/j.archoralbio.2016.09.014>
- Wakabayashi S, Koide T (2011) Histidine-rich glycoprotein: a possible modulator of coagulation and fibrinolysis. *Semin Thromb Hemost* 37:389–394. <https://doi.org/10.1055/s-0031-1276588>
- Kolte D, Shariat-Madar Z (2016) Plasma Kallikrein inhibitors in cardiovascular disease an innovative therapeutic approach. *Cardiol Rev* 24:99–109. <https://doi.org/10.1097/CRD.0000000000000069>
- Schmaier AH, McCrae KR (2007) The plasma kallikrein-kinin system: its evolution from contact activation. *J Thromb Haemost* 5:2323–2329. <https://doi.org/10.1111/j.1538-7836.2007.02770.x>
- Niemeier A, Schinke T, Heeren J, Amling M (2012) The role of apolipoprotein E in bone metabolism. *Bone* 50:518–524. <https://doi.org/10.1016/j.bone.2011.07.015>
- Rivera-Chacon DM, Alvarado-Velez M, Acevedo-Morantes CY et al (2013) Fibronectin and vitronectin promote human fetal osteoblast cell attachment and proliferation on nanoporous titanium surfaces. *J Biomed Nanotechnol* 9:1092–1097. <https://doi.org/10.1166/jbn.2013.1601>

32. Ru D-W, Yan Y-F, Li B et al (2016) Tetranectin knock-out mice exhibit features of kyphosis and osteoporosis. *Fudan Univ J Med Sci* 43:159. <https://doi.org/10.3969/j.issn.1672-8467.2016.02.006>
33. Albrektsson T, Johansson C (2001) Osteoinduction, osteoconduction and osseointegration. *Eur Spine J* 10:96–101. <https://doi.org/10.1007/s005860100282>
34. Martínez-Ibáñez M, Murthy NS, Mao Y et al (2017) Enhancement of plasma protein adsorption and osteogenesis of hMSCs by functionalized siloxane coatings for titanium implants. *J Biomed Mater Res Part B Appl Biomater* 106:1138–1147. <https://doi.org/10.1002/jbm.b.33889>

## Affiliations

**N. Araújo-Gomes<sup>1,2</sup> · F. Romero-Gavilán<sup>1</sup>  · I. García-Arnáez<sup>3</sup> · C. Martínez-Ramos<sup>2</sup> · A. M. Sánchez-Pérez<sup>2</sup> · M. Azkargorta<sup>4</sup> · F. Elortza<sup>4</sup> · J. J. Martín de Llano<sup>5</sup> · M. Gurruchaga<sup>3</sup> · I. Goñi<sup>3</sup> · J. Suay<sup>1</sup>**

<sup>1</sup> Departamento de Ingeniería de Sistemas Industriales y Diseño, Universitat Jaume I, Av. Vicent-Sos Baynat s/n, 12071 Castellón, Spain

<sup>2</sup> Department of Medicine, Universitat Jaume I, Av. Vicent-Sos Baynat s/n, 12071 Castellón, Spain

<sup>3</sup> Facultad de Ciencias Químicas, Universidad del País Vasco, P. M. de Lardizábal, 3, 20018 San Sebastián, Spain

<sup>4</sup> Proteomics Platform, CIC bioGUNE, CIBERehd, ProteoRed-ISCIH, Bizkaia Science and Technology Park, 48160 Derio, Spain

<sup>5</sup> Department of Pathology, Faculty of Medicine and Dentistry, Health Research Institute of the Hospital Clínico (INCLIVA), University of Valencia, 46010 Valencia, Spain